Puroindoline-b Mutations Control the Lipid Binding Interactions in Mixed Puroindoline-a:Puroindoline-b Systems†

Luke A. Clifton,‡,§ Rebecca J. Green,§ and Richard A. Frazier*,‡

Department of Food Biosciences and Reading School of Pharmacy, University of Reading, PO Box 226, Whiteknights, Reading RG6 6AP, U.K.

Received August 20, 2007; Revised Manuscript Received October 3, 2007

ABSTRACT: The interactions have been investigated of puroindoline-a (Pin-a) and mixed protein systems of Pin-a and wild-type puroindoline-b (Pin-b+) or puroindoline-b mutants (G46S mutation (Pin-bH) or W44R mutation (Pin-bS)) with condensed phase monolayers of an anionic phospholipid (L-α-dipalmitoylphosphatidyl-*dl*-glycerol (DPPG)) at the air/water interface. The interactions of the mixed systems were studied at three different concentration ratios of Pin-a:Pin-b, namely 3:1, 1:1 and 1:3 in order to establish any synergism in relation to lipid binding properties. Surface pressure measurements revealed that Pin-a interaction with DPPG monolayers led to an equilibrium surface pressure increase of 8.7 ± 0.6 mN m^{-1}. This was less than was measured for Pin-a:Pin-b+ (9.6 to 13.4 mN m^{-1}), but was significantly more than was measured for Pin-a:Pin-bH (4.0 to 6.2 mN m^{-1}) or Pin-a:Pin-bS (3.8 to 6.3 mN m^{-1}) over the complete range of concentration ratio. Consequently, surface pressure increases were shown to correlate to endosperm hardness phenotype, with puroindolines present in hard-textured wheat varieties yielding lower equilibrium surface pressure changes. Integrated amide I peak areas from corresponding external reflectance Fourier-transform infrared (ER-FTIR) spectra, used to indicate levels of protein adsorption to the lipid monolayers, showed that differences in adsorbed amount were less significant. The data therefore suggest that Pin-b mutants having single residue substitutions within their tryptophan-rich loop that are expressed in some hard-textured wheat varieties influence the degree of penetration of Pin-a and Pin-b into anionic phospholipid films. These findings highlight the key role of the tryptophan-rich loop in puroindoline−lipid interactions.

Puroindolines are basic, cysteine rich, water soluble proteins found in the seed endosperm of wheat (var. *Triticum aestivum*) (*1*, *2*), and are the major constituents of friabilin (*3*), the group of proteins that is found bound to the surface of water washed wheat starch. They exist as two isoforms, puroindoline-a (Pin-a[1]) and puroindoline-b (Pin-b), which exhibit 55% homology in their sequence, and share lipid binding properties that are attributed to a tryptophan-rich structural loop enclosed by a disulfide bond (*4*−*6*). This loop is a unique feature of the puroindolines and features a domain containing 5 tryptophan residues in Pin-a in the sequence WRWWKWWK, which is truncated to 3 tryptophan residues in Pin-b in the sequence WPTKWWK. The puroindolines have attracted particular attention for their role in determining wheat endosperm texture (*3*, *7*, *8*), an important end-use quality parameter for wheat, and for their potential antimicrobial and antifungal activity (*1*, *9*−*11*).

In hexaploid wheat varieties the gene coding the puroindolines is linked to the *Hardness* locus (*Ha*) on the short arm of chromosome 5D (*12*, *13*), which has been shown to control endosperm texture. The texture of the endosperm is fundamental to the milling quality of wheat and defines its end use; hard milling wheat is more suitable for bread, whereas soft milling wheat is suitable for cakes and biscuits. The wheat wild-type is soft textured, and hard wheat varieties contain either null forms or mutated forms of the genes controlling the expression of Pin-a and Pin-b. This was first reported by Giroux and Morris (*14*), who discovered a G46S point mutation on the Pin-b gene (*Pinb-D1b*) of several hard varieties, which occurred within the tryptophan-rich loop (enclosed by a disulfide bond between C29 and C48 in Pin-b). The expression of this Pin-b mutant in wheat was later demonstrated to have a causative role in the hard texture of several hard wheat varieties (*15*). Further altered alleles of the puroindolines were later reported, either encoding mutation near or within the tryptophan-rich loop for Pin-b (L60P and W44R point mutations) or stopping the synthesis of Pin-a or Pin-b altogether (*16*, *17*).

Despite the well-documented genetic evidence for the role of puroindolines in endosperm texture, the exact biochemical mechanism remains unclear. In hard wheat varieties, strong adhesion is observed between starch granules and the

† This work was supported by the U.K. Biotechnology and Biological Sciences Research Council (Studentship BBSSA200411018).

* To whom correspondence should be addressed. Tel: +44 118 3788709. Fax: +44 118 9310080. E-mail: r.a.frazier@reading.ac.uk.

‡ Department of Food Biosciences.

§ Reading School of Pharmacy.

[1] Abbreviations: CMC, carboxymethylcellulose; DPPG, dipalmitoylphosphatidyl-*dl*-glycerol; ER-FTIR, external reflection Fourier transform infrared; HPLC, high performance liquid chromatography; Pin-a, puroindoline-a; Pin-b, puroindoline-b; Pin-b+, wild-type Pin-b; Pin-bH, Pin-b with G46S mutation; Pin-bS, Pin-b with W44R mutation; PTFE, polytetrafluoroethylene; SDS−PAGE, sodium dodecyl sulfate−polyacrylamide gel electrophoresis; UHQ, ultra-high quality.

10.1021/bi701680w CCC: $37.00
Published on Web 11/07/2007

surrounding protein matrix within the endosperm, whereas in soft wheat varieties the adhesion is weak. Localization studies of the mature starchy endosperm show that both puroindolines are present in the protein matrix and, critically, at the interface between this matrix and starch granules (*3*, *18*). It has been suggested that the presence of puroindolines on the surface of starch granules could be lipid mediated (*6*), since this interface has been shown to contain lipid membrane remnants (*19*), and because the puroindolines can be extracted from the wheat endosperm only by using detergents (*1*), which suggests that they are lipid-bound *in vivo*.

In a recent paper (*20*), we demonstrated that the Pin-b wild-type found in soft textured wheat varieties and two mutated forms of this protein found in hard textured wheat varieties (having either a G46S substitution or W44R substitution) show different behavior during adsorption at the air/water and condensed phase anionic phospholipid monolayer interfaces. In particular, mutated Pin-b forms exhibited reduced insertion within anionic phospholipid monolayers. Here the behavior of Pin-a at these interfaces is examined together with the effect of the presence of these three Pin-b forms on the adsorption behavior. Pin-a and Pin-b are found colocalized on the starch surface in wheat and Pin-b has recently been shown to control Pin-a starch binding in the wheat endosperm (*21*). Therefore, the effect to which the Pin-b mutants found in hard wheat varieties affect Pin-a activity compared to that of wild-type Pin-b will give further information on the biochemical causes of wheat endosperm texture.

MATERIALS AND METHODS

Materials. L-α-Dipalmitoylphosphatidyl-*dl*-glycerol (DPPG, synthetic purity >99%) was purchased from Avanti Polar Lipids (Alabaster, AL) and was used without further purification. Stock solutions (1 g dm^{-3}) of DPPG were prepared in HPLC grade chloroform (Sigma-Aldrich, Dorset, U.K.) and stored at room temperature, with 1:2 dilutions of these solutions being used experimentally. Puroindoline proteins were extracted from wheat flour and purified using Triton X-114 phase partitioning and chromatographic techniques as described in the next section. All other chemicals were sourced from Sigma-Aldrich and were of the highest purity available.

For surface pressure measurements, protein solutions (0.1 g dm^{-3}) were prepared in phosphate buffer solution (Na_2HPO_4 and NaH_2PO_4 at total ionic strength, $I = 0.02$ M) at pH 7 using UHQ grade water. For ER-FTIR spectroscopy, protein stock solutions (0.1 g dm^{-3}) were prepared in D_2O phosphate buffer solution at pH 7 ($I = 0.02$ M). Solutions used in ER-FTIR spectroscopy experiments were prepared 24 h in advance to allow sufficient H−D exchange (*22*). Mixed puroindoline solutions were prepared from stock single protein solutions and allowed to equilibrate at room temperature for 1 h prior to experimentation.

Puroindoline Purification. Pin-a was extracted and purified from the Claire wheat variety. Wild-type Pin-b (Pin-b+), Pin-bH (G46S substitution) and Pin-bS (W44R substitution) were extracted and purified from the wheat varieties Claire, Hereward and Soissons, respectively. The procedure used is detailed below and was that described by Day *et al.* (*23*) as a modification of the procedure first reported by Kooijman *et al.* (*24*).

Wheat flour (480 g) was mixed with PEK buffer (0.05 M sodium phosphate, pH 7.6, 5 mM ethylenediaminetetraacetic acid, 0.05 M KCl; 2.4 dm^3) at 4 °C for 1 h. Once centrifuged (3500*g*, 10 min) the pellet was extracted with 4% (v/v) Triton X-114 in PEK buffer (1.2 dm^3) at 4 °C for 2 h. After centrifugation (13000*g*, 10 min), the pellet was discarded and the pH of the supernatant was adjusted to 4.5 with glacial acetic acid. Carboxymethylcellulose (CMC, 24 g) was added to the Triton X-114 solution, and this was stirred at 4 °C for 12 h. After centrifugation (13000*g*, 10 min), the pellet was washed with 0.05 M acetic acid solution (800 cm^3, ×2). The supernatant and pellet were both retained for further steps to yield Pin-a and Pin-b as described below.

Pin-a. The supernatant TX-114 solution was heated to 30 °C for 30 min, and the resulting solution was centrifuged at 13000*g* for 10 min. The detergent rich phase was mixed with a 1:3 ether:ethanol (2.4 dm^3) and stored at −20 °C for ∼18 h to allow the protein to precipitate. The solution was then centrifuged at 13000*g* for 10 min, and the pellet was then washed twice and dried in air. The dried pellet was then redissolved in 0.05 mol acetic acid solution and then dialyzed against this (2 × 5 dm^3) at 4 °C for 48 h prior to lyophilizing.

Pin-b. The CMC pellet-bound proteins were eluted with 1 M NaCl in 0.05 M acetic acid (160 cm^3) at 4 °C for 1 h. Following filtration to remove the CMC, 28 g of NaCl was added to the filtrate. After mixing for 1 h and centrifugation (13000*g*, 10 min), the pellet was dissolved in 0.05 M acetic acid (40 cm^3) and dialyzed against 0.05 M acetic acid (2 × 5 dm^3, 48 h), then lyophilized.

Cation Exchange Chromatography. Separation of the puroindolines from the crude protein extracts was then carried out using a preparative Mono-S HR 16/10 cation exchange column (Pharmacia Biotech UK, Buckinghamshire, U.K.) and a BioCad Sprint perfusion chromatography system (Global Medical Instruments, Minneapolis, MN). The sample was prepared by dissolving lyophilized crude protein (60 mg) in 2.5 cm^3 of 0.05 M ammonium acetate 25% (v/v) acetonitrile pH 5.5, heating at 30 °C for 30 min prior to centrifugation (3500*g*, 10 min) and filtration.

The CMC-bound and unbound protein fractions were eluted over a gradient of 0.05−1 M ammonium acetate, pH 5.5, 25% (v/v) acetonitrile. The flow rate was constant at 3 $cm^3\ min^{-1}$, and the absorbance was monitored at 280 nm. The Pin-a fraction was eluted from the CMC-unbound extract at 0.4 M ammonium acetate concentration, and the Pin-b fraction was eluted at 0.6 M ammonium acetate concentration. Fractions were dialyzed against deionized water (5 dm^3, for 48 h, refreshed every 24 h) and lyophilized. The purity and identity of the lyophilized Pin-b fraction was confirmed using SDS−PAGE (*25*) and capillary electrophoresis (*23*). The proteins were stored at −20 °C until used.

Surface Pressure Measurements. Surface pressure measurements were carried out using a polytetrafluoroethylene (PTFE) Langmuir trough (94 × 22 × 5 mm), and the surface pressure monitored *via* a Wilhelmy plate surface pressure sensor (Nima Technology, Coventry, U.K.). To create lipid monolayers at the air/water interface, the PTFE trough was filled with 7.5 cm^3 of 0.02 M phosphate buffer (pH 7). Five microliters of lipid solution (0.5 g dm^{-3}) was spread at the

air/water interface and compressed using a single barrier to a surface pressure of 22 mN m^{-1}. The compressed lipid films were monitored via pressure (π) vs time measurements to check the stability of these films. A 0.5 cm^3 sample of the appropriate 0.1 g dm^{-3} puroindoline solution was then added to the aqueous subphase to give a final concentration of 6 μg cm^{-3} (0.46 μM). Change in the surface pressure as a result of puroindoline adsorption was monitored by plotting surface pressure vs time, keeping the layer compression (area) constant for a total of 260 min. Equilibrium surface pressure changes were measured in triplicate experiments as the difference in surface pressure at equilibrium (nominally at $t = 260$ min) and surface pressure of the lipid film before introduction of protein to the aqueous subphase. One way analysis of variance was performed to test for differences in the surface pressure change data at $p < 0.05$, followed by the determination of least significant difference by the Tukey test also at $p < 0.05$ (*26*). Analysis of variance was performed within selected groups of data to test the effect of mixing Pin-a with each Pin-b variant in turn, as well as to determine any differences between the different mixed systems.

FTIR Spectroscopy. ER-FTIR spectra were recorded using a ThermoNicolet Nexus instrument (Madison, WI) fitted with a monolayer/grazing angle accessory (Specac 19650 series, Kent, U.K.), a mercury cadmium telluride detector, and an air dryer to purge the instrument of water vapor and carbon dioxide. Lipid−protein interactions were analyzed by external reflectance using the method described by Lad *et al.* (*27*). The accessory was equipped with a PTFE trough (same dimensions as that used for surface pressure measurements) and barrier for the preparation of compressed lipid layers. All spectra were recorded at a resolution of 4 cm^{-1} where 256 interferograms were collected, co-added, and ratio-ed against the buffer.

During each experiment, 7.5 cm^3 of D_2O phosphate buffer ($I = 0.02$ M, pH 7) was placed in the trough and the single beam background spectra were recorded after allowing time for the sample chamber to purge H_2O and CO_2. After recording background spectra, 5 μL of a 0.5 g dm^{-3} lipid solution was added to the buffer surface and then compressed to the predefined 22 mN m^{-1} condensed phase position determined using surface pressure measurements. Sample scans were taken to ensure the stability of the lipid film and checked via the observation of the symmetric and asymmetric CH_2 stretching of the lipid chain at 2854−2850 cm^{-1} and 2924−2916 cm^{-1}, respectively. A 0.5 cm^3 sample of a 0.1 g dm^{-3} protein solution was then added to the aqueous subphase without disturbing the lipid monolayer, to give a final concentration of 6.25 μg cm^{-3} (0.48 μM). Spectra were continuously taken from the moment of protein introduction to the system for the initial 15 min of the experiment followed by 1 spectrum per 15 min thereafter. Spectra were recorded for a total of 260 min. The interaction of the protein with the lipid monolayer was observed via monitoring the amide I band at approximately 1650 cm^{-1} and the lipid acyl chain vibrations (approximately 2920 and 2850 cm^{-1}). Protein adsorption to the bare air/water interface was carried out using the above method without the presence of the lipid monolayer.

All spectra were corrected for complete removal of the H_2O and HOD peaks from the amide spectral region. To correct for water vapor, H_2O and HOD spectra were scaled and subtracted against each protein spectrum. The degree of subtraction depended on absorption time and H/D exchange. The HOD spectra were recorded during the purge of the air/liquid sample area prior to addition of the lipid film (*27*). No further processing was carried out.

FTIR transmission spectra of protein solutions were recorded using a deuterium triglyceride sulfate detector. Protein solutions were made to a concentration of 2 mg cm^{-3} (154 μmol dm^{-3}) in D_2O phosphate buffer ($I = 0.02$ M, pH 7) and placed in a Specac Omni liquid cell (Specac, Kent, U.K.) fitted with CaF_2 windows and a Mylar spacer to give a path length of 6 μm. Spectra were collected as interferograms at 4 cm^{-1} resolution, where 64 interferrograms were collected, co-added and ratio-ed against a background spectrum of the buffer solution.

The Fourier self-deconvolution process was performed on the amide I peaks of the protein spectra using the instrument software. The bandwidth was kept constant for each spectrum. The resulting bands are not "real" and therefore solely used as a qualitative comparison tool.

Table 1: Surface Pressure Changes for Puroindoline Interactions with Lipid and Air/water Interfaces

puroindoline type/mix	surface pressure change/mN m^{-1} DPPG	surface pressure change/mN m^{-1} air/water
Pin-a	8.7 ± 0.6	11.6 ± 0.3
Pin-b+	10.6 ± 1.0[a]	12.8 ± 0.1[a,b]
1:3 Pin-a:Pin-b+	10.3 ± 0.8	
1:1 Pin-a:Pin-b+	11.7 ± 1.7[b]	13.0 ± 0.2[b]
3:1 Pin-a:Pin-b+	9.9 ± 0.5	
Pin-bH	7.9 ± 1.6[a]	12.4 ± 0.1[a,b]
1:3 Pin-a:Pin-bH	5.0 ± 1.0[c]	
1:1 Pin-a:Pin-bH	5.9 ± 0.5[b]	11.6 ± 0.3[d]
3:1 Pin-a:Pin-bH	3.8 ± 0.3[c]	
Pin-bS	6.3 ± 1.0[a,b]	11.5 ± 0.3[a]
1:3 Pin-a:Pin-bS	5.3 ± 1.0[b]	
1:1 Pin-a:Pin-bS	4.3 ± 0.5[c]	12.7 ± 0.5[c]
3:1 Pin-a:Pin-bS	5.0 ± 0.1[b]	

[a] Data previously reported in ref (*20*). [b] Significant difference ($p < 0.05$) with respect to surface pressure changes for Pin-a as a single protein within column. [c] Significant difference ($p < 0.05$) with respect to surface pressure changes for constituent Pin-a and Pin-b proteins as single proteins within column. [d] Significant difference ($p < 0.05$) with respect to surface pressure changes for Pin-bH as a single protein within column.

RESULTS

Puroindoline Adsorption to the Air/Water Interface. The adsorption to the air/water interface of Pin-a alone and Pin-a mixed with Pin-b+, Pin-bH or Pin-bS was monitored by surface pressure measurements and ER-FTIR spectroscopy. These experiments were performed with the aim to characterize the surface activity of Pin-a, and any changes in its surface activity brought about by the presence of Pin-b proteins in solution. A comparison of the surface activity of the three differing Pin-b proteins has been reported previously (*20*), and is summarized by the surface pressure data shown in Table 1.

Figure 1A shows the surface pressure isotherm (surface pressure vs time) for the adsorption of Pin-a at the bare air/

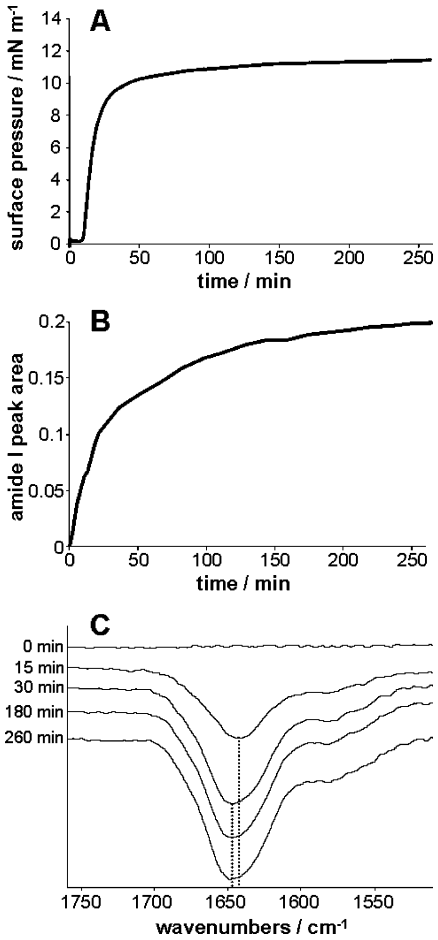

FIGURE 1: (A) Surface pressure isotherms, (B) integrated Pin-a amide I peak area plots, and (C) corresponding raw Pin-a amide I band spectra, all recorded during the adsorption of Pin-a to the air/water interface. The dotted lines in C show the shift in the peak maxima of the amide I band during the adsorption process from 1645 cm^{-1} to 1648 cm^{-1}.

water interface. Surface pressure was observed to increase rapidly due to Pin-a adsorption after an induction period of 9 min, giving an overall surface pressure increase of 11.6 ± 0.3 mN m^{-1}. Induction periods in surface pressure isotherms do not necessarily indicate an absence of adsorption, and 50% molecular surface coverage of protein at the air/water interface can be required before a change in surface pressure is detected (*28*). Indeed, Figure 1B shows the corresponding plot of the integrated amide I peak area vs time for Pin-a adsorption to the air/water interface that shows evidence of Pin-a adsorption during the surface pressure induction period. Figure 1C shows the amide I band spectral region raw data recorded at various time points from 0 to 260 min after Pin-a was introduced to the solution subphase. The initial amide I band showed a peak maximum at 1645 cm^{-1}, which was shifted to 1648 cm^{-1} at about 30 min after Pin-a addition, indicating an increased α-helix content.

Figure 2A shows the surface pressure isotherms for protein adsorption to the air/water interface from the three mixed Pin-a:Pin-b systems (all 1:1 ratio of each protein). For each of the mixed systems there was no induction period prior to the observation of a surface pressure increase, which was in contrast to the behavior of Pin-a as a single protein. Adsorption of Pin-a:Pin-b+ (1:1) yielded an equilibrium pressure increase of 13.0 ± 0.2 mN m^{-1}, while Pin-a:Pin-bS (1:1) and Pin-a:Pin-bH (1:1) gave equilibrium surface pressure increases of 12.7 ± 0.5 mN m^{-1} and 11.6 ± 0.3 mN m^{-1}, respectively. One way analysis of variance revealed that there were significant differences among the data, although only for the Pin-a:Pin-bS mixed system was there a significant difference to the behavior of both Pin-a and Pin-bS. In the other mixed systems the behavior was apparently dominated by one isoform.

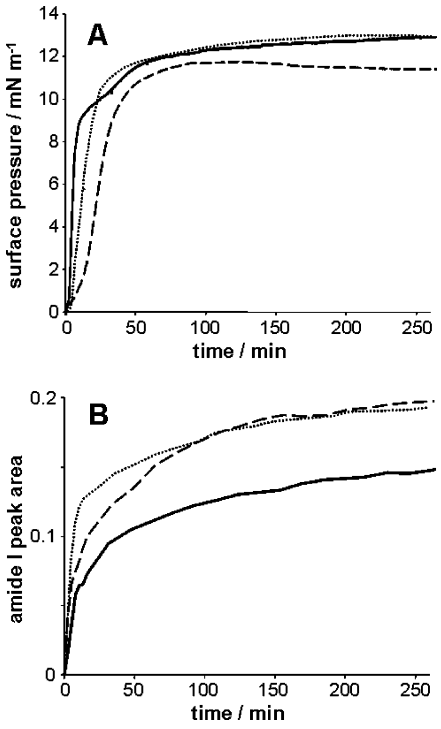

FIGURE 2: (A) Surface pressure isotherms and (B) integrated amide I peak areas recorded during adsorption to the air/water interface from 1:1 mixed puroindoline (Pin-a:Pin-b) solutions. The solid line represents Pin-a:Pin-b+, the dashed line represents Pin-a:Pin-bH, and the dotted line represents Pin-a:Pin-bS.

ER-FTIR spectroscopy enabled a comparison of the relative amounts of protein adsorbed at the interface as shown in Figure 2B. The three mixed Pin-a:Pin-b systems in all cases gave an amide I band with a peak maximum at 1643 cm^{-1} (spectra not shown), which showed no significant shift during the adsorption process. The amide I peak area (an indicator of adsorbed amount) of protein at the interface was revealed to be dependent on the Pin-b type. The mutant forms of Pin-b mixed with Pin-a yielded the greatest adsorption (peak area), with approximately equal final peak areas for Pin-a:Pin-bS and Pin-a:Pin-bH. Pin-b+ mixed with Pin-a yielded a final peak area that was 25% less than those for the mutants. Although the final amount of protein seen at the air/water interface for adsorption from Pin-a:Pin-b+ was apparently less than for the mutant mixtures, this did not coincide with a reduced equilibrium surface pressure change for this adsorption process.

Puroindoline Adsorption to Anionic Phospholipid (DPPG) Monolayers. Figure 3A shows the surface pressure isotherm recorded after the addition of Pin-a to the aqueous subphase in the presence of a DPPG monolayer. The interaction of Pin-a with this monolayer resulted in an equilibrium surface pressure increase of 8.7 ± 0.6 mN m^{-1}, with the surface pressure isotherm exhibiting two steps as previously observed for the interaction of wild-type Pin-b with DPPG monolayers

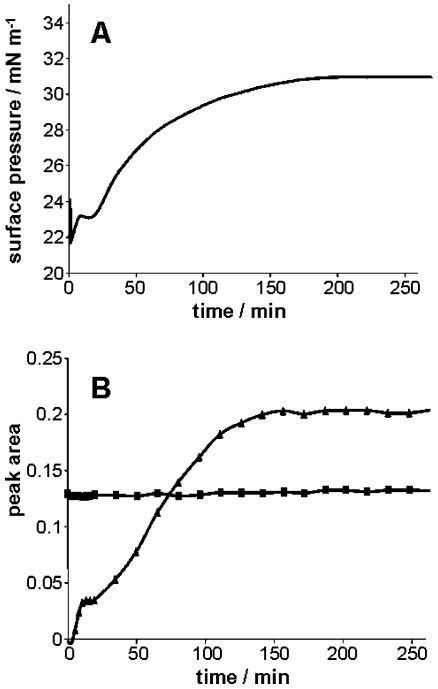

FIGURE 3: (A) Surface pressure isotherms, and (B) integrated peak area plots of (▲) amide I band (1650 cm^{-1}) and (■) DPPG CH_2 asymmetric stretch (2920 cm^{-1}) from ER-FTIR spectra recorded during the interaction of Pin-a with condensed phase monolayers of DPPG.

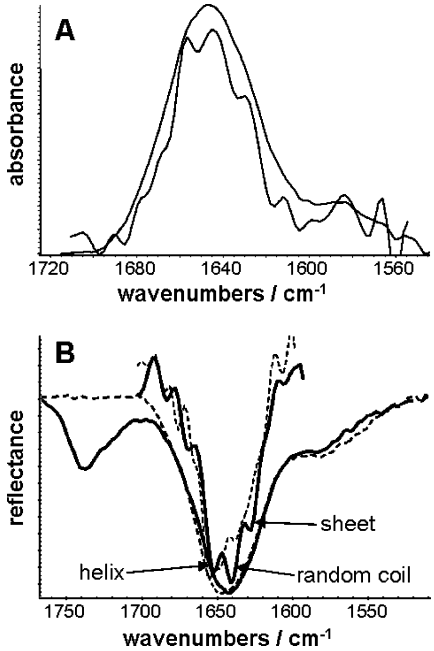

FIGURE 4: Amide I regions and deconvoluted amide I bands from (A) transmission FTIR spectra of Pin-a in solution at pH 7, and (B) ER-FTIR spectra of Pin-a at the air/water (dashed lines) and DPPG lipid (solid line) interfaces.

(*20*). The first step reached a steady state after approximately 10 min, and the second step, which is associated with the majority of the surface pressure increase, commenced after approximately 20 min and reached equilibrium 150 min after Pin-a introduction. Figure 3B shows the corresponding data from ER-FTIR spectroscopy. The increase in amide I peak area also shows a distinct two-step adsorption isotherm over similar time scales. No change to the lipid acyl CH_2 stretches was observed, suggesting no significant change in orientation and order of the lipid layer during protein adsorption.

Figure 4 shows the protein amide I band for Pin-a in solution (Figure 4A) and adsorbed at the air/water interface with and without the presence of a DPPG monolayer (Figure 4B). Pin-a shows a similar secondary structure when adsorbed to the lipid film as when in solution, with the bands at 1644 cm^{-1} showing structural elements which agree with those reported by Le Bihan *et al.* (*29*). The final adsorbed structure at the air/water interface shows differing secondary structure to that for Pin-a in solution or at the lipid interface, being predominantly α-helix in structure, with the contribution of both the random coil and *β*-sheet elements being lower compared to those for both the solution and lipid adsorbed structure.

Figure 5 shows the surface pressure isotherms for the adsorption of the three mixed Pin-a:Pin-b systems to DPPG monolayers at different ratios of each protein, namely 1:3, 1:1 and 3:1. The equilibrium surface pressure changes recorded in these isotherms are summarized in Table 1. All puroindoline mixes and ratios showed evidence of insertion into the DPPG monolayers, as evidenced by surface pressure increases. Pin-a:Pin-b+ gave the highest equilibrium surface pressure increase at each ratio, with the increase at a 1:1 ratio being the highest overall. The Pin-a:Pin-b mutant systems exhibited similar surface pressure isotherms at each protein ratio, as well as both yielding significantly lower equilibrium surface pressure increases to Pin-a:Pin-b+ systems at all ratios of the constituent proteins. Analysis of variance showed that there was no significant effect of mixing Pin-a with Pin-b+, i.e., the equilibrium surface pressure changes at the three ratios of Pin-a:Pin-b+ were not significantly different to those for Pin-a or Pin-b+ as single proteins. In contrast, when mixed with Pin-bH or Pin-bS there was a significant reduction in the equilibrium surface pressure change with respect to the constituent single proteins at all protein ratios except 1:1 Pin-a:Pin-bH, which was not significantly different to Pin-bH, 1:3 and 3:1 Pin-a:Pin-bS, which were not significantly different to Pin-bS. At certain Pin-a:Pin-bH and Pin-bS ratios, a decrease in surface pressure was observed in the surface pressure profiles after 150 min, but no corresponding decrease in the amide I peak area was observed in ER-FTIR spectra (Figure 6). It is therefore suggested that these phenomena in surface pressure data were associated with a rearrangement of the protein at the lipid interface, with protein inserted being excluded from the condensed phase lipid monolayer film and moving to become adsorbed below the monolayer.

Figure 6 shows the corresponding plots of the integrated amide I band and CH_2 peak areas (associated with the protein and lipid acyl chain regions respectively) against time during the adsorption of mixed puroindoline systems to DPPG monolayers. During all experiments there was no change in the bands associated with the DPPG monolayer, with the lipid CH_2 asymmetric stretch maintaining a consistent peak area of approximately 0.13, suggesting no loss of lipid from the interface. At the 1:3 and 1:1 Pin-a:Pin-b ratios (Figures 6A and 6B, respectively) there was little apparent difference in the final equilibrium adsorption of protein at the interface, albeit that there were some differences in the rates of

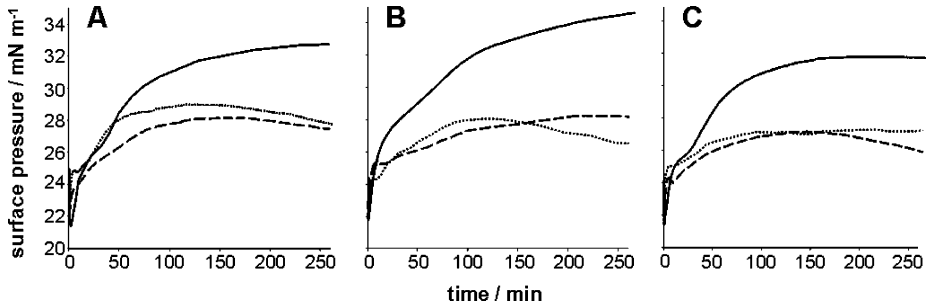

FIGURE 5: Surface pressure isotherms for the interaction of mixed Pin-a:Pin-b systems with condensed phase DPPG monolayers. Differing puroindoline ratios of (A) 1:3, (B) 1:1 and (C) 3:1 Pin-a:Pin-b are shown in the respective plots. The solid line represents Pin-a:Pin-b+, the dashed line represents Pin-a:Pin-bH, and the dotted line represents Pin-a:Pin-bS.

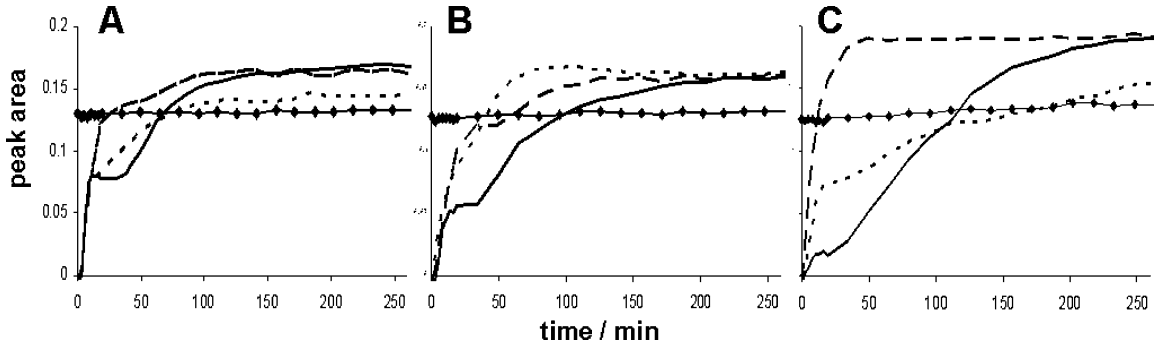

FIGURE 6: Integrated peak areas of the (◆) lipid CH_2 asymmetric stretch (2920 cm^{-1}) and protein amide I band (1650 cm^{-1}) recorded during the interaction of Pin-a:Pin-b+ (solid line), Pin-a:Pin-bH (dashed line) and Pin-a:Pin-bS (dotted line) at three differing Pin-a:Pin-b ratios, (A) 1:3, (B) 1:1 and (C) 3:1 Pin-a:Pin-b.

adsorption and therefore the shapes of the adsorption isotherms.

The most defined differences in adsorption across the three Pin-b types were noted for the 3:1 Pin-a:Pin-b mixed systems (Figure 6C). At this ratio Pin-a:Pin-bH showed the most rapid adsorption, reaching equilibrium within 40 min of protein introduction at a larger peak area than reached at the other ratios studied. Pin-a:Pin-b+ gave a similar equilibrium amide I peak area to Pin-a:Pin-bH, which again was higher than at the other ratios for this system; but the absorption process was much slower, the two step process not reaching equilibrium adsorption until 240 min after introduction of the puroindolines to the solution subphase. Pin-a:Pin-bS exhibited rapid adsorption over the first 10 min, followed by slow adsorption, which did not appear to reach equilibrium within the experimental time period. The generally higher adsorption of protein from 3:1 Pin-a:Pin-b mixed systems may have been due to the excess of Pin-a present at this ratio as the adsorbed amounts were similar to those observed for Pin-a (Figure 3B).

The final amide I peak maxima of the lipid adsorbed puroindolines were similar for each system at each ratio (data not shown) with 1:3, 1:1 and 3:1 Pin-a:Pin-b having maxima at 1641, 1642 and 1643 cm^{-1} respectively. The peak maxima were between the range of values for Pin-a and Pin-b individually, which show lipid adsorbed amide I peak maxima at 1644 and 1640 cm^{-1}, respectively (*20*).

DISCUSSION

Pin-a Interactions at Air/Water and Lipid Interfaces. At the bare air/water interface, Pin-a showed slower adsorption and a significantly lower equilibrium surface pressure than has been observed for wild-type Pin-b (*20*), which indicates that Pin-a is less surface active in agreement with surface pressure data reported by Biswas *et al.* (*30*). This difference in surface activity between Pin-a and Pin-b may partly be due to Pin-a undergoing conformational change during this adsorption process as revealed by ER-FTIR spectra (Figure 4), leading to an increase in α-helix content accompanied by a relative loss of random coil and β-sheet compared to the solution structure of the protein. In contrast, Pin-b was shown not to undergo a significant structural shift during its surface adsorption, but did conversely show an increase in β-sheet content at the lipid interface (*20*). The difference in behavior between Pin-a and Pin-b may be related to differences in the structure of these isoforms, particularly the variation in the tryptophan-rich loop. However, this is uncertain given the lack of knowledge on their three-dimensional solution structures, of which a better understanding is needed (*31*).

When adsorbing to the anionic DPPG lipid interface, Pin-a does not appear to undergo structural change, with the lipid adsorbed and the solution structure appearing similar, and helix, sheet and random coil components of the secondary structure being approximately similar to those reported by Le Bihan *et al.* (*29*) (Figure 4). The adsorption of Pin-a to the lipid interface was shown by both ER-FTIR spectroscopy and surface pressure measurements to occur *via* a two step adsorption process, that was similar to that observed for Pin-b+ adsorbing to the same lipid interface. Although Pin-a apparently shows a higher final amount of adsorbed protein at this interface according to integrated amide I peak areas than was observed for wild-type Pin-b, it conversely shows a lower amount of insertion into the monolayer, as indicated by the surface pressure measurements (Table 1). It is thus suggested that Pin-a shows a larger amount of adsorption

FIGURE 7: Primary structure amino acid sequences of (1) Pin-b+, (2) Pin-bH mutant (G46S) and (3) Pin-bS mutant (W44R) based on sequence analysis by Gautier *et al.* (*2*). The tryptophan-rich loop is highlighted in bold in each protein and is formed by a disulfide bond between C29 and C48.

under, rather than into the lipid monolayer, with the majority of the adsorbed protein remaining in solution (thus retaining its solution secondary structure) either interacting with the anionic head group of DPPG or aggregating with other Pin-a molecules. Since the surface pressure and ER-FTIR data both reveal two steps to the adsorption process, it is suggested that the initial step is monodisperse single protein adsorption into the film and the second step is aggregation around these inserted proteins, giving aggregated bodies of Pin-a within, but mainly under the DPPG monolayer, as was reported by Dubriel *et al.* (*4*). The reason for the difference in insertion to anionic lipid monolayers between Pin-a and Pin-b remains unclear, although the relative higher insertion of Pin-b into anionic lipid monolayers does agree with previously reported data that suggested Pin-b has a higher affinity for anionic phospholipids than Pin-a (*5*). The differing tryptophan content in the tryptophan-rich loops of Pin-a and Pin-b will cause this important structural element of Pin-a to be inherently more hydrophobic than that of Pin-b, which may explain why a higher final amount of Pin-a adsorbs at the lipid interface. The higher antimicrobial activity of Pin-b compared to Pin-a noted by Capperelli *et al.* (*32*) may be related to the observed differences in anionic lipid insertion ability, with Pin-b better able to permeate microbial membranes than Pin-a.

Mixed Puroindoline Systems. The adsorption from mixed 1:1 Pin-a:Pin-b solutions to the air/water interface showed distinct differences to the behavior of the constituent proteins. The data in Figure 2 demonstrated a dependence of the adsorption from each mixed system on the Pin-b type present, and a comparison of surface pressure changes between mixed and single protein systems (Table 1) suggests synergistic activity. Pin-bS is the least surface active of the three Pin-b types studied here (*20*) and has similar surface activity to Pin-a; however, Pin-a:Pin-bS was more surface active than either Pin-bS or Pin-a. In terms of equilibrium surface pressure increase and rate of increase, the Pin-a:Pin-b+ system exhibited similarity to the isotherms observed for Pin-b+ as a single protein, although the final absorbed amount (indicated by amide I peak area) was significantly less than for any other mixed puroindoline system. Adsorption from Pin-a:Pin-bH solutions gave adsorption trends and equilibrium surface pressure changes similar to those observed for Pin-a as a single protein. This may suggest the dominance of Pin-a in this system, although no significant shift in the amide I peak maximum was seen as had been observed for Pin-a singularly. In fact, in all cases of 1:1 mixed puroindoline adsorption to the bare air/water interface, an amide I peak with a maximum of 1643 cm^{-1} was observed, which may suggest that the large structural change apparent during Pin-a adsorption does not occur when Pin-a is mixed with Pin-b.

The data for the interaction of mixed puroindolines with DPPG lipid monolayers reveal differing lipid binding behavior as a result of the single residue substitutions within the tryptophan-rich loops of Pin-b+, Pin-bH and Pin-bS. The extent of lipid monolayer penetration (indicated by surface pressure increase in Figure 5) was significantly less for the Pin-a:Pin-bH and Pin-a:Pin-bS mixed systems in comparison to Pin-a:Pin-b+ at all Pin-a:Pin-b ratios. In contrast, ER-FTIR spectroscopy data (Figure 6) did not show major differences in the amounts of protein adsorbing from the different mixed systems at 1:3 and 1:1 Pin-a:Pin-b ratios. Although there were some differences in adsorption rates according to Pin-b type at the 3:1 Pin-a:Pin-b ratio according to ER-FTIR spectroscopy, these did not correlate to the behavior exhibited in surface pressure data. This suggests that amount of puroindoline insertion to DPPG monolayers was not dependent on amounts of protein adsorbed below the monolayer. ER-FTIR spectra indicated that in all cases both Pin-a and Pin-b adsorb to the lipid monolayer, since the peak maximum of the amide I band of the mixed puroindolines at the lipid interface is at the midpoint between that of Pin-a and Pin-b as single proteins. This appears to exclude the possibility that the differences in lipid monolayer penetration observed were linked to an exclusion of either protein from the interface.

The equilibrium surface pressure change for mixed Pin-a:Pin-b+ was similar to that of Pin-b+ as a single protein at all Pin-a:Pin-b+ ratios, yet the equilibrium surface pressure changes for Pin-a mixed with either of the Pin-b mutants were less than those measured for either the Pin-b mutants as single proteins (see Table 1) or Pin-a. It is therefore suggested that the combination of Pin-a with these mutants leads to an inhibition of lipid monolayer insertion, with the protein adsorbing mainly under the lipid film with only a very small amount of the protein penetrating into the film. This inhibitory effect would imply synergistic activity between Pin-a and the Pin-b mutants, and highlights different behavior between puroindolines obtained from soft wheat varieties (Pin-a with Pin-b+) and puroindoline types present in hard wheat varieties where Pin-b is present in a mutated

form (Pin-a with Pin-bH or Pin-bS). Indeed, it is interesting to note that the Pin-a:Pin-b mutant mixed systems exhibit very similar lipid binding interactions in terms of equilibrium surface pressure increases.

The data presented here and in previous work (*20*) provide *in vitro* evidence that single residue substitutions within the tryptophan-rich loop of Pin-b (Figure 7) have a significant influence on the interaction between puroindolines and lipids in the presence of Pin-a as well as in its absence. This influence of Pin-b mutations is not as significant for adsorption to the air/water interface, which highlights the key role of the tryptophan-rich loop in puroindoline-lipid interactions and especially in the adsorption-insertion process to lipid interfaces. As discussed in our earlier work (*20*), the G46S mutation in Pin-bH introduces a more polar serine residue that is more likely to participate in hydrogen-bonding side-chain interactions and is also more bulky than glycine, resulting in a net loss of conformational freedom in the tryptophan-rich loop that may hinder lipid layer penetration. In the case of the W44R mutation in Pin-bS, the substitution causes an increase in positive charge and a reduction to the hydrophobicity of the loop. The basic arginine residue is more likely to interact with the polar head group of the lipid, thus favoring adsorption instead of lipid layer penetration. Since the interaction with a synthetic model lipid has been studied, it is not possible to conclude on the precise mechanisms involved in the relationships between puroindolines and endosperm hardness. However, the results presented here do suggest a significant role of protein−lipid and protein−protein interactions in determining the hardness character of the wheat endosperm, and further suggest that the levels of puroindolines found on the surface of starch granules in the wheat endosperm could indeed be lipid mediated (*6*).

ACKNOWLEDGMENT

We thank Campden & Chorleywood Food Research Association for the donation of wheat flour samples.

REFERENCES

1. Blochet, J.-E., Chevalier, C., Forest, E., Pebay-Peyroula, E., Gautier, M.-F., Joudrier, P., Pézolet, M., and Marion, D. (1993) Complete amino acid sequence of puroindoline, a new basic and cystine-rich protein with a unique tryptophan-rich domain, isolated from wheat endosperm by Triton X-114 phase partitioning, *FEBS Lett. 329*, 336−340.
2. Gautier, M.-F., Aleman, M.-E., Guirao, A., Marion, D., and Joudrier, P. (1994) *Triticum aestivum* puroindolines, two basic cystine-rich seed proteins: cDNA sequence analysis and developmental gene expression, *Plant Mol. Biol. 25*, 43−57.
3. Greenwell, P., and Schofield, J. D. (1986) A starch granule protein associated with endosperm softness in wheat, *Cereal Chem. 63*, 379−380.
4. Dubreil, L., Vie, V., Beaufils, S., Marion, D., and Renault, A. (2003) Aggregation of puroindoline in phospholipid monolayers spread at the air-liquid interface, *Biophys. J. 85*, 2650−2660.
5. Dubriel, L., Compoint, J.-P., and Marion, D. (1997) Interaction of puroindolines with wheat flour polar lipids determines their foaming properties, *J. Agric. Food Chem. 45*, 108−116.
6. Greenblatt, G. A., Bettge, A. D., and Morris, C. F. (1995) Relationship between endosperm texture and occurrence of friabilin and bound polar lipids on wheat starch, *Cereal Chem. 72*, 172−176.
7. Jolly, C. J., Rahman, S., Kortt, A. A., and Higgins, T. J. V. (1993) Characterisation of the wheat Mr 15 000 "grain softness protein" and analysis of the relationship between its accumulation in the whole seed and grain softness, *Theor. Appl. Genet. 86*, 589−597.
8. Morris, C. F., Greenblatt, G. A., Bettge, A. D., and Malkawi, H. I. (1994) Isolation and characterization of multiple forms of friabilin, *J. Cereal Sci. 21*, 167−174.
9. Charnet, P., Molle, G., Marion, D., Rousset, M., and Lullien-Pellerin, V. (2003) Puroindolines form ion channels in biological membranes, *Biophys. J. 84*, 2416−2426.
10. Krishnamurthy, K., Balconi, C., Sherwood, J. E., and Giroux, M. J. (2001) Wheat puroindolines enhance fungal disease resistance in transgenic rice, *Mol. Plant-Microbe Interact. 14*, 1255−1260.
11. Faize, M., Sourice, S., Dupuis, F., Parisi, L., Gautier, M. F., and Chevreau, E. (2004) Expression of wheat puroindoline-b reduces scab susceptibility in transgenic apple (*Malus x domestica Borkh.*), *Plant Sci. 167*, 347−354.
12. Mattern, P. J., Morris, R., Schmidt, J. W., and Johnson, V. A. (1973) Location of genes for kernal properties in wheat variety 'Cheyenne' using chromosome substitution lines, in *Proceedings of the 4th International Wheat Genetics Symposium*, pp 703−708, University of Missouri−Columbia.
13. Sourdille, P., Perretant, M. R., Charmet, G., Leroy, P., Gautier, M.-F., Joudrier, P., Nelson, J. C., Sorrells, M. E., and Bernard, M. (1996) Linkage between RFLP markers and genes affecting kernel hardness in wheat, *Theor. Appl. Genet. 93*, 580−586.
14. Giroux, M. J., and Morris, C. F. (1997) A glycine to serine change in puroindoline b is associated with wheat grain hardness and low levels of starch-surface friabilin, *Theor. Appl. Genet. 95*, 857−864.
15. Beecher, B., Bettge, A., Smidansky, E., and Giroux, M. J. (2002) Expression of wild-type pinB sequence in transgenic wheat complements a hard phenotype, *Theor. Appl. Genet. 105*, 870−877.
16. Giroux, M. J., Talbert, L. E., Habernicht, D. K., Lanning, S., Hemphill, A., and Martin, J. M. (2000) Association of puroindoline sequence type and grain hardness in hard red spring wheat, *Crop Sci. 40*, 370−374.
17. Martin, J. M., Frohberg, R. C., Morris, C. F., Talbert, L. E., and Giroux, M. J. (2001) Milling and bread baking traits associated with puroindoline sequence type in hard spring wheat, *Crop Sci. 41*, 228−234.
18. Dubreil, L., Gaborit, T., Bouchet, B., Gallant, D. J., Broekaert, W. F., Quillien, L., and Marion, D. (1998) Spatial and temporal distribution of the major isoforms of puroindolines (puroindoline-a and puroindoline-b) and nonspecific lipid transfer protein (ns-LTP1e$_1$) of *Triticum aestivum* seeds. Relationships with their in vitro antifungal properties, *Plant Sci. 138*, 121−135.
19. Al-Saleh, A., Marion, D., and Gallant, D. J. (1986) Microstructure of mealy and vitreous wheat endosperms (*Triticum durum L.*) with special emphasis on location and polymorphic behaviour of lipids, *Food Microstruct. 5*, 131−140.
20. Clifton, L. A., Lad, M. D., Green, R. J., and Frazier, R. A. (2007) Single amino acid substitutions in puroindoline-b mutants influence lipid binding properties, *Biochemistry 46*, 2260−2266.
21. Swan, C. G., Meyer, F. D., Hogg, A. C., Martin, J. M., and Giroux, M. J. (2006) Puroindoline b limits binding of puroindoline a to starch and grain softness, *Crop Sci. 46*, 1656−1665.
22. Green, R. J., Hopkinson, I., and Jones, R. A. L. (1999) Unfolding and intermolecular association in globular proteins adsorbed at interfaces, *Langmuir 15*, 5102−5110.
23. Day, L., Bhandari, D. G., Greenwell, P., Leonard, S. A., and Schofield, J. D. (2006) Characterization of wheat puroindoline proteins, *FEBS J. 273*, 5358−5373.
24. Kooijman, M., Orsel, R., Hessing, M., Hamer, R. J., and Bekkers, A. C. A. P. A. (1997) Spectroscopic characterisation of the lipid-binding properties of wheat puroindolines, *J. Cereal Sci. 26*, 145−159.
25. Laemmli, U. K., and Favre, M. (1973) Maturation of the head of bacteriophage T4 DNA packaging events, *J. Mol. Biol. 80*, 575−599.
26. Armitage, P. (1971) *Statistical Methods in Medical Research*, pp 189−207, Blackwell Scientific, Oxford.
27. Lad, M. D., Birembaut, F., Frazier, R. A., and Green, R. J. (2005) Protein-lipid interactions at the air/water interface, *Phys. Chem. Chem. Phys. 7*, 3478−3485.
28. Tripp, B. C., Magda, J. J., and Andrade, J. D. (1995) Adsorpion of globular proteins at the air/water interface as measured via dynamic surface tension: concentration dependence, mass-transfer considerations, and adsorption kinetics, *J. Colloid Interface Sci. 173*, 16−27.

29. Le Bihan, T., Blochet, J.-E., Désormeaux, A., Marion, D., and Pézolet, M. (1996) Determination of the secondary structure and conformation of puroindolines by infrared and Raman spectroscopy, *Biochemistry 35*, 12712−12722.

30. Biswas, S. C., Dubriel, L., and Marion, D. (2001) Interfacial behavior of wheat puroindolines: study of adsorption at the air-water interface from surface tension measurements using Wilhelmy plate method, *J. Colloid Interface Sci. 244*, 245−253.

31. Marion, D., Bakan, B., and Elmorjani, K. (2007) Plant lipid binding proteins: Properties and applications, *Biotechnol. Adv. 25*, 195−197.

32. Capparelli, R., Amoroso, M. G., Palumbo, D., Iannaccone, M., Faleri, C., and Cresti, M. (2005) Two plant puroindolines colocalize in wheat seed and in vitro synergistically fight against pathogens, *Plant Mol. Biol. 58*, 857−867.

BI701680W